

N75 19189

PILOT PERFORMANCE DURING A SIMULATED STANDARD  
INSTRUMENT PROCEDURE TURN WITH AND WITHOUT  
A PREDICTOR DISPLAY

John G. Kreifeldt<sup>1</sup> • Thomas Wempe<sup>2</sup>

(1) Tufts University  
Medford Mass. 02155

(2) Ames Research Center, NASA  
Moffett field, Calif. 94035

SUMMARY

A simulator study was conducted to measure the effectiveness of predictor information incorporated into a CRT display of a computer simulated aircraft's horizontal and vertical situation. Professional pilots served as subjects for the task of executing a standard instrument procedure turn at constant altitude in constant crosswinds with and without their predicted ground track displayed.

The results showed that the display with the predicted ground track was markedly and significantly superior to the display without this information and that the subjects were generally satisfied with this type of information. Mean rms lateral path error was independent of the crosswind velocity with the predictor information, and increased without it with increasing wind velocity. Rms stick activity decreased with the predictor display which also "uncoupled" aileron and elevator activity.

This research is part of a general investigation into the effectiveness of pictorial displays for manual control and monitoring at NASA-Ames, Man/Machine Integration Branch.

INTRODUCTION

It is sure that the future of commercial aviation will be marked by increasing pressure for tighter spatial and temporal flight constraints on individual aircraft as well as introduction of complex trajectories particularly for V/STOL aircraft. This pressure will be necessary for reasons of density, economy, safety and consideration of public human factors such as noise abatement and area exclusions.

The human's role in the aircraft in the coming decades is still to be determined but clearly it may vary from direct manual involvement in piloting to a flight management type of position in which the human may, among other functions, monitor automatic systems and operate as a goal setter and multiperformance evaluator. (For discussion of

such possibilities see Warner<sup>(1)(2)</sup>.) It is sure that the total flight system will be optimized by researching and exploiting the best man-machine match.

A primary difficulty in man-machine system design is providing adequate information to the human in an easily assimilable form. This is true whether the human has direct ("inner-loop") manual involvement or system monitoring responsibility. Complete operational man-machine systems have a tendency to meet acceptable performance standards until they fail catastrophically with a very steep transition between these two phases. Much of this characteristic can be traced to man's limited mental information processing capabilities and limited prediction ability.

It has been shown numerous times that the Ziebold-Paynter<sup>(3)</sup> philosophy of predicting the behavior of an operating dynamic system and feeding this information back for use in the system can radically improve total system performance. Kelley has extended this technique to feeding back to the human a visual display of the predicted performance of the dynamic system. This has resulted in marked and significant improvements in controlling systems such as submarines and aircraft. Much of the use of this technique and philosophy is discussed by Kelley<sup>(4)</sup>.

This report discusses a simulation experiment in which professional pilot-subjects flew a standard procedure turn in crosswinds using horizontal and vertical attitude information presented on a CRT. The turn was "flown" with and without predicted ground path information displayed on the CRT in order to gain objective and subjective evaluation of the effect of a predictor display in a simple routine task. (Work along this line is also being pursued at Boeing by Warner<sup>(5)</sup>.)

The predicted path consisted of a solid line extending from the aircraft symbol center out to a time length of 30 seconds. The physical length of this line depends upon the aircraft attitude, velocity and the strength of the crosswinds. The path shape is determined by the equations used to compute each predicted position but generally is responsive to winds and aircraft attitude also. As in all predictor displays, the farther forward in time the prediction is made, the more sensitive it becomes to operator and environmental influences incorporated into the prediction equations. Thus the "tail" of the predicted path can have disturbing movements. However, the thirty second prediction span used in this experiment did not seem to be excessive given the generally smooth control used by the subjects. The thirty second span was chosen so that its length under zero crosswind conditions was sufficient to "fair-in" the flight path through regions in which the actual path was inferable but not actually displayed.

PRECEDING PAGE BLANK NOT FILMED

Altitude and elevator control was available but not rudder nor throttle control.

#### PREDICTOR MATHEMATICS

As originally formulated by Ziebolz & Paynter, the behavior of a "plant" can be predicted over some time span or at some interval by modeling the plant dynamics and (by suitable scaling) running this simulation plant in fast-time (or "speeded-up") with the same inputs to both actual and fast-time plant. Actually, a number of subtle approximations enter into this philosophy such as the assumed behavior of the plant inputs over the future time being predicted and the plant dynamics model used.

This may be put into context by considering the functional block diagram of the A/C and display system equations as used in this experiment. Figure 1 shows the system in its essential form of human operator, A/C dynamics, Euler transformations and ground coordinate transformations. Notice for example that gusts are input to the A/C constant crosswinds are input to the ground coordinate transformations.

In this experiment, only the  $x, y$ , values were predicted and combined to display a future ground track. Any of the output quantities could be predicted and displayed, in principle.

#### PREDICTOR EQUATIONS

There are several ways of predicting the ground coordinates. The most direct method is to consider a series like expansion of the outputs assuming that, in fact, this is possible. The Taylor series expansion for  $x$  using  $t$  as the present time and  $\tau$  as the future time would look like:

$$x(t, \tau) = x(t) + x'(t) \cdot \tau + x''(t) \cdot \frac{\tau^2}{2!} + \dots$$

$$x''(t) = \text{initial condition at time } t \quad (1)$$

$$x(t, \tau) = \text{predicted value at time } (t + \tau)$$

In principle this assumes  $x(t)$  to be analytic. It is not clear without experiments how far to carry out the expansion in order for the displayed values of  $x(t, \tau)$  to be useful as a prediction. This approach has, in fact, been used by Dey<sup>(6)(7)</sup> in single point predictions with the series terminated after the squared term: the advantage

of this method is the avoidance of any A/C dynamics modelling and direct measurability of the coefficients. A disadvantage is that direct knowledge of the environment and its future behavior such as winds is not used to best advantage.

A next approach would be to move further back along the path and express  $x$  as a function of the winds ( $W_x$ ) and the inputs to the ground coordinate transformations. At this point either Taylor series approximations to  $\theta, \psi, \phi$ , could be used or assumptions made about their behavior. Again, if series approximations are used, knowledge about the A/C dynamics, wind gusts and controller movements is not utilized.

Therefore, at any stage, one has the choice of basing output predictions on:

- (1) (Taylor) series approximation (extrapolation) of the outputs
  - (2) assumed behavior of the inputs with consequent transformation
  - (3) expression of the inputs as a function of inputs to the previous block
  - (4) assumed behavior of the output.
- Obviously, option (3) simply moves consideration of (1) and (2) back to a prior block.

In order to be more specific and reveal some similarities and differences in (1) and (2), the specific A/C dynamics and approximations of the experiment will be used. To simplify matters and to correspond to the actual experiment which did not use  $z$  (altitude) prediction, only prediction of  $x$  and  $y$  will be considered.

The equations used in the experiment to simulate the dynamics of a Navion single-engine, four-place light aircraft are given below.

$$\dot{p} = L_p \cdot p + L_{\delta_a} \cdot \delta_a$$

$$\dot{r} = (S/U_0) \cdot p$$

$$\begin{bmatrix} \dot{u} \\ \dot{v} \\ \dot{q} \end{bmatrix} = \begin{bmatrix} X_u & X_w & -S/S \\ Z_u & Z_w & U_0 \\ 0 & M_w & M_q \end{bmatrix} \begin{bmatrix} u \\ v \\ q \end{bmatrix} + \begin{bmatrix} 0 \\ 0 \\ M_{\delta_a} \end{bmatrix} \cdot \delta_a \quad (2)$$

The main approximations in this simulation were:

- (1) Throttle control not used.
- (2) Wind gusts not present.
- (3) Coordinated turns for small bank angles.
- (4) Rudder control not used.
- (5) Pitch angle ( $\theta$ ) generally less than  $20^\circ$ .

Thus the pilot-subject always made coordinated turns, and only had aileron ( $\delta_a$ ) and elevator ( $\delta_e$ ) control.

The numerical coefficients can be found in the Appendix and are the same as used by Palmer and Wempe<sup>(8)</sup> in a previous report.

The Euler transform approximations and ground coordinate transforms are shown in Equation 3 producing only pitch rate ( $\dot{\theta}$ ) and yaw rate ( $\dot{\psi}$ ) needed for x, y positions. These x, y coordinates were displayed as the instantaneous position of the A/C on the horizontal situation display (HSD).

#### APPROXIMATE EULER TRANSFORMS

$$\dot{\theta} = q \cdot \cos \phi - r \sin \phi$$

$$\dot{\psi} = q \cdot \sin \phi + r \cos \phi$$

$$\dot{\phi} = p - \frac{U_0}{g} \cdot \dot{r}$$

(3)

#### APPROXIMATE GROUND TRANSFORMS

$$\dot{x} = U_0 \cdot \cos \theta \cdot \cos \psi + W_x$$

$$\dot{y} = U_0 \cdot \cos \theta \cdot \sin \psi + W_y$$

$$\dot{z} = U_0 \cdot \sin \theta + (W + 0.05236 U_0) \cdot \cos \psi$$

#### Predictor Equations for Simulation

Two further simplifying assumptions were made in establishing the predictor equations. The pitch angle ( $\theta$ ) in inertial coordinates was assumed small enough that  $\cos \theta$  was nearly unity. This is not a severe restriction since a pitch angle of  $20^\circ$  produces only a 6% deviation from unity. In addition, the bank angle ( $\phi$ ) was also assumed to be less than  $20^\circ$  with the same result. In the actual dynamic simulation, the bank angle for a standard turn rate of  $3^\circ/\text{sec}$  would be about  $16^\circ$ . With these approximations made for the predictor equations, the set of equations in (3) reduces to the following necessary set.

$$\begin{aligned} \dot{\psi} &= r \\ \dot{r} &= p \cdot g/U_0 \\ \dot{p} &= L_p \cdot p + L_{\delta_a} \cdot \delta_a \end{aligned} \quad \begin{aligned} \dot{x} &= U_0 \cdot \cos \psi + W_x \\ \dot{y} &= U_0 \cdot \sin \psi + W_y \end{aligned} \quad (4)$$

The predicted results will be in error to the extent that these assumptions are violated in the simulation.

Assuming  $\delta_a$  as the input and  $\psi$  as the output,  $\psi$  can be written in Laplace and time domain form as:

$$\begin{aligned} \psi(s) &= \frac{\psi_0}{s} + \frac{r_0}{s^2} + \frac{p_0}{U_0} \cdot \frac{1}{s^2(s-L_p)} + L_{\delta_a} \cdot \frac{\delta_a(s)}{U_0} \cdot \frac{1}{s^2(s-L_p)} \\ \psi(t) &= \psi_0 + r_0 \cdot t + \frac{g \cdot p_0}{U_0} \left[ \frac{e^{L_p t}}{L_p^2} - \frac{1}{L_p^2} - \frac{t}{L_p} \right] + \mathcal{L}^{-1} \left\{ L_{\delta_a} \cdot \frac{\delta_a(s)}{U_0} \cdot \frac{1}{s^2(s-L_p)} \right\} \end{aligned} \quad (5)$$

The first three terms depend only upon initial conditions of yaw angle ( $\psi_0$ ), yaw rate ( $r_0 = \dot{\psi}_0$ ) and roll rate ( $p_0$ ). The last terms depend upon the behavior of the aileron control ( $\delta_a$ ). For demonstration purposes, the simplistic assumption can be made that  $\delta_a$  does not change but maintains a value of  $D$  over the prediction interval. Then after gathering terms together, and noting that prediction intervals will be longer than 1 second:

$$\frac{L_p t}{e^{L_p t}} \approx 0 \quad t > 1 \text{ sec.} \quad (L_p = -0.402 \text{ sec}^{-1}) \quad (6)$$

then

$$\begin{aligned} \psi(t) &= \psi_0 - \frac{g/U_0}{L_p} (p_0 + (-\frac{L_p}{L_p})D) + t \cdot [r_0 - \frac{g/U_0}{L_p} (p_0 + (-\frac{L_p}{L_p})D)] \\ &\quad - \frac{t^2}{2} \left[ \frac{g}{U_0} (-\frac{L_p}{L_p}) D \right] \end{aligned} \quad (7)$$

It is instructive to compare this exact terminating equation for  $\psi(t)$  with the Taylor series approximation based upon its instantaneous derivatives.

$$\psi(t) = \psi_0 + \psi'_0 \cdot t + \psi''_0 \cdot \frac{t^2}{2} + \psi'''_0 \cdot \frac{t^3}{3} + \dots \quad (8)$$

A direct term-by-term identity of (7) and (8) is not obviously possible.

One could make nearly any assumption about aileron controller movement ( $\delta_a$ ) over the prediction interval. The more complicated it becomes the higher the order terms in (7). However, a fairly reasonable assumption made for this experiment was that  $\delta_a$  is zero over the prediction interval, or in other words, the pilot would fly in a zero stick position. Thus the actual equation used for prediction extrapolation was

$$\psi(t) = \psi_0 - \frac{g/U_0}{L_p^2} \cdot P_0 + t \left[ r_0 - \frac{g/U_0}{L_p} \cdot P_0 \right] \quad (9)$$

$\psi_0$  = initial yaw angle

$P_0$  = initial roll rate

$r_0$  = initial yaw rate

It may be puzzling that in the above equation (9)

$$\psi(0) \neq \psi_0 \quad (10)$$

however, (9) is not valid at  $t = 0$  because of neglect of the exponential term (equation (6)). Equation (9) is equivalent to assuming that the yaw rate is constant.

#### Displayed Equations.

Equation (9) was used to predict the values of  $x$ ,  $y$  from time  $t$  (now) to  $(t + \tau)$  by obtaining the initial condition values at  $t$  and transforming to ground coordinates.

$$\psi(t, \tau) = \left[ \psi(t) - \frac{g/U_0}{L_p^2} \cdot p(t) \right] + \tau \cdot \left[ r(t) - \frac{g/U_0}{L_p} \cdot p(t) \right] \quad (11)$$

$$\Delta \alpha_0(t) + \alpha_1(t) \cdot \tau$$

$$\dot{x}(t, \tau) = W_x + U_0 \cdot \cos \psi(t, \tau) \quad x(t, 0) = X(t) \quad (12)$$

$$\dot{y}(t, \tau) = W_y + U_0 \cdot \sin \psi(t, \tau) \quad y(t, 0) = Y(t)$$

yielding

$$\begin{aligned} x(t, \tau) &= W_x \cdot \tau + \frac{U_0}{\alpha_1} \cdot \sin \left[ \alpha_0(t) + \alpha_1(t) \cdot \tau \right] \\ &+ \left[ x(0) - \frac{U_0}{\alpha_1} \sin \alpha_0(t) \right] \\ y(t, \tau) &= W_y \cdot \tau - \frac{U_0}{\alpha_1} \cdot \cos \left[ \alpha_0(t) + \alpha_1(t) \cdot \tau \right] \\ &+ \left[ y(0) + \frac{U_0}{\alpha_1} \cos \alpha_0(t) \right] \end{aligned} \quad (13)$$

In order to reduce computation, the predicted path coordinates ( $x$ ,  $y$ ) were computed and displayed for every other second into the future from  $\tau = 2$  to  $\tau = 30$  seconds with straight lines connecting the points. These predictions were updated 20 times per second with the effect that the assumption of zero aileron control was offset by picking up new initial conditions frequently enough.

These approximations and display conditions seemed to produce a satisfactory looking result inasmuch as the predicted path always started from the present position, had no "kinks" in it and moved smoothly. A very slight ripple could sometimes be discerned in the path due to the updating frequency and the amount of deviation of each temporal path point from its previous position.

It is clear from the equations used in (11) and (12) that if  $\psi(t, r)$  is non-zero constant over the prediction interval, a straight line predicted path results while if  $\psi(t, r)$  is a non-zero constant, second order curves will result. In general, the higher the order of  $\psi(t)$ , the higher the path order.

#### EXPERIMENTAL DESCRIPTIONS

##### Instrumentation

The basic instrumentation used for the experiment was a two axes fingertip side arm displacement controller with spring centering, a start-stop button, a SEL 816A CRT and SEL 840MP computer. Figure 2 shows the CRT and controller at the subject's position. During a test, a 6' high screen enclosed the subject and display.

The digital computer calculated the A/C dynamic responses, the predictor information, all display elements and transformations and recorded the raw data for later analysis. A functional block diagram of the experimental setup is shown in Figure 3.

##### Task and Display Elements

The task to be performed was the execution of a 180° procedure turn at constant altitude with a crosswind of 0%, 10%, or 20% of the nominal A/C forward velocity. This task was executed with and without predicted path information so that each subject received 6 different conditions (3 x 2). The crosswind always blew at constant velocity in the direction shown in Figure 4.

A map-like display of the desired A/C path projected onto a horizontal ground plane was displayed along with the A/C symbol and predicted path (when used). This information constituted the horizontal situation display (HSD). The vertical situation display (VSD), positioned directly above the HSD, contained the following 6 information display elements: an A/C wing symbol stationary in the middle of the VSD with the movable artificial horizon in an inside-out configuration; an error box centered on the A/C symbol in compensatory fashion for zero lateral and altitude error when on the correct course; a turn rate indicator with bars marking 0°, ±3°/sec.; and altitude and velocity information. Figure 4 is a labeled photograph of the HSD and VSD information display elements.

A brief word about the standard turn path. The circular arcs that should actually be flown between the linear portions are suppressed in order to decrease the correction and display required.

Instead, the curved portions were boxed by their tangent lines and both the A/C symbol and the error box flashed on and off briefly when the A/C (projected back to the path) entered the turning point.

The map was stationary and the A/C moved so that the A/C was primarily head-down over most of the flight. Thus, there were times of control-display incompatibility for the HSD inasmuch as a right bank head motion would produce a left turning display motion of the head-down A/C.

Since the procedure turn is flown by time rather than distance, the actual size of the map is relatively immaterial and was made as large as feasible within the HSD.

The predicted future path of the A/C was added as a projected ground track 30 seconds long. Inasmuch as the crosswind was also entered into the prediction equations, the predicted path changed in length and curvature in response to the wind as well so that it might appear very short or very elongated. Figures 5a, b, and c show sample appearances of this predicted path. Notice in Figure 5b the yaw angle of the A/C while still on the path. The dynamics were adjusted to make only coordinated turns.

##### Subjects and Test Procedure

Six experienced airline pilots served as subjects. Their flight experience is summarized in Table I. None had used predictor displays before.

TABLE I  
PILOT EXPERIENCE

PILOT	POSITION	AIRCRAFT	Experience (hours)	
			Simulator with Visual & Hood with Inst. Only	Total Flight Time
1	Captain	B747	210	8,350
2	Co-Pilot	B707	1,150	3,600
3	Captain	B720	325	15,350
4	1st Officer	B707	150	4,070
5	Flight Officer	B707	500	6,350
6	2nd Officer	B727	(No data reported)	3,000

A subject would, on his test day, fly either with or without the predictor receiving four runs of each wind condition in a randomized order for a total of 12 runs per day, with a short rest after every 4 runs. Each subject received one day of practice without the predictor and one day of practice with the predictor with three runs each of the randomized wind conditions for practice. Three subjects practiced with the predictor first. The test days were likewise balanced for predictor-no predictor use. Practice and test conditions were independent.

#### Performance Measures

(1) The main performance measures were the mean and rms values of the lateral and altitude path errors; (2) elevator and aileron stick activities in the form of rms deflections were also recorded with (3) the total flight time also taken as secondary item of interest. (4) A short pilot-opinion questionnaire about the experiment was given to each subject to fill out after his series of tests was completed. (5) The actual lateral paths were also recorded for visual inspection later in order to study the efficacy of the predictor information.

#### RESULTS AND DISCUSSION

##### Lateral and Height RMS Errors

[All results are based upon data from 5 subjects. The sixth subject's data which conformed to the trends shown had several extremely large error scores for the no predictor case and was judged atypical in several other ways and was, therefore, eliminated from the comprehensive results.]

The major results can be seen in Figure 6 which compares the rms lateral offset and rms height error with and without the ground track predictor display.

Two results are apparent in Figure 6.

1. While the average values of the rms errors tend to increase in the no predictor case with increasing winds, the average rms errors are lower and are independent of the crosswinds with the predictor display.

2. The variation about each mean value also appears smaller with the predictor display.

This figure indicates that when the predicted horizontal ground track was displayed, performance on the altitude holding task improved as well even though no altitude prediction was displayed. There was an average decrease in rms lateral error of 110% and an average decrease of 64% in the rms height when using the predictor display. Table II summarizes the reduced data for these two error scores.

TABLE II

Reduced Data for the Lateral and Altitude Offset Errors With and Without the Predictor Display During a Standard Instrument Procedure Turn

Predictor Display	Crosswind Velocity + Aircraft Velocity						
	0.0		0.1		0.2		
	On	Off	On	Off	On	Off	
Mean rms score (ft)	149.2	285.9	149.9	301.4	143.3	343.2	Lateral Offset
% Difference	91		101.1		139.5		
Significance Level (1)	>99.0		>99.0		>99.9		
S.D. of the rms scores (ft)	29.0	76.2	48.4	105.1	40.1	120.5	
Significance of S.D. (2)	>99.9		>99.9		>99.9		Altitude Offset
Mean rms score (ft)	14.0	18.4	14.9	22.6	13.9	28.8	
% Difference	31.4		51.7		107.2		
Significance level (1)	<90.0		>90.0		>99.0		
S.D. of the rms scores (ft)	4.2	6.7	7.3	10.2	5.8	23.0	
Significance of S.D. (2)	Not Significant		Not Significant		>99.0		

Data based on 5 subjects

(1) Fisher F Test - 13 D.F.

(2)  $\chi^2$  Test - 1 D.F.

Thus, there is a beneficial carry over of the horizontal predictor display element to the vertical situation as well. It is probably safe to conclude that the improvement in altitude performance using

the horizontal predictor display is attributable to both decreased attention loading on the horizontal display and less horizontal maneuvering leading to less vertical interaction. In the first case, more attention can be directed toward the vertical situation display and in the second case, fewer corrective actions need to be taken.

The correlation ( $\rho$ ) between the lateral and height errors was .91 and .88 for the predictor - no predictor case respectively with no significant difference and each correlation was significant past the 99.9% level. Thus, a high lateral error score corresponded to a high height error score with and without the predictor element.

One could conclude, that if the predicted ground track is displayed, lateral offset information on the VSD could most likely be eliminated with a consequent savings in computation/display requirements and an uncluttering of the VSD.

#### Stick Activity

Aileron ( $\delta_a$ ) and elevator ( $\delta_e$ ) movements of the controller were also sampled during the flights and the mean and rms values obtained. The rms values (in arbitrary units) measure a pilot's stick activity and are an indirect indication of the sizes and frequency of corrective actions and the "smoothness" of the flight.

Figure 7 shows the general behavior of the two activities with and without the predictor element.

As with the lateral and height errors, both the average activities and the variance of the activities were significantly lower where the predicted ground track was displayed. Aileron activity dropped by 64% while elevator activity dropped by 42%. The reduced data for the stick activities are shown in Table III.

TABLE III

Reduced Data for the Elevator and Aileron RMS Stick Activity During a Standard Instrument Procedure Turn

Predictor Display	Crosswind Velocity + Aircraft Velocity						
	0.0		0.1		0.2		
	On	Off	On	Off	On	Off	
Mean rms score (ft)	.61	.85	.61	.87	.59	.85	Elevator
% Difference (1)	3.95		41.4		45.2		
Significance level	<90.0		<90.0		>90.0		
S.D. of the rms scores (ft)	.12	.38	.25	.39	.21	.45	Activity $\delta_a$
Mean rms score	.79	1.20	.73	1.25	.69	1.17	Aileron
% Difference (1)	51.1		71.2		70.6		
Significance level	>90.0		>90.0		>95.0		
S.D. of the rms scores	.22	.53	.16	.54	.21	.49	Activity $\delta_e$

Data based on 5 subjects  
(1) Fisher F Test - 13 D.F.

As Figure 7 indicates, there was no apparent wind effect on stick activity with or without the predictor display and a reduction in activity with the horizontal predictor element carried over from the horizontal to the vertical situation.

The average correlation between aileron and elevator stick activities was surprisingly high for the no predictor case ( $\rho = .97$ , significant at the 99.9% level) and rather lower ( $\rho = .67$ , significant at the 99% level) with the predictor. Introduction of the predictor element, therefore, seems to "uncouple" somewhat the two tasks of maintaining altitude and path. This decrease in correlation in the stick activities with the predictor display is unexpected since the lateral

and height errors were fairly highly correlated with each other with and without the predictor display.

#### Stick Activities and Errors

As might be expected, rms height error and elevator stick activity are strongly correlated with and without the predictor ( $p = .94$  and  $.92$ , significant beyond the 99.9% level) with no significant difference between the two conditions. This is reasonable since an altitude error is either introduced or corrected by elevator stick movement generally.

On the other hand, rms lateral error and aileron stick activity were weakly correlated with and without the predictor (.26 and .39 respectively, not significant at the 95% level). This also is expected since following the turn exactly would still require appreciable aileron activity.

#### Flight Times

The flight times increased linearly with increasing crosswind velocity as would be expected. The theoretical minimum time to fly the path would be 225 seconds as the course was displayed. The average time, using the predictor display, ranged from 230.9 seconds in zero wind to 248.5 seconds in a 20% wind. The times were slightly longer without the predictor display, being 234.8 sec. to 249.5 for the above wind conditions. The relatively small dependence on the wind can be attributed to its direction relative to the path. The wind generally aided as much as delayed the flight except for the very initial leg. The extra time without the predictor can be attributed to the error path generally being longer than the actual one.

#### Anecdotal Information

The subjects were generally more relaxed using the predictor display which was easily observed by noting the set of their shoulders, and their body distance from the display. With no predictor, the subjects tended to lean in to the CRT and also raise their shoulders, denoting a stressful condition. The subjects seemed also to show more forearm muscle stiffness after the no predictor flights.

One subject, an experienced airline pilot, had difficulty flying the simulation without the predictor element. However, with the predictor element his performance was typical of the group's.

All the subjects were highly cooperative and generally enthusiastic about participating. Several expressed a desire to have similar

predictor elements incorporated into their actual flight displays.

#### SUMMARY OF RESULTS

The major results may be summarized as follows:

1. Introduction of the predicted ground track into the HSD decreased mean rms error scores and their variances for both lateral offset and altitude deviation.
2. The predictor element caused the mean rms lateral offset and altitude error scores to be constant and independent of the crosswinds.
3. Aileron and elevator stick activity decreased significantly as well with introduction of the predictor element. Stick activity remained essentially constant for the different crosswinds with and without the predictor element.
4. The predictor element "uncoupled" the aileron and elevator activities by nearly half.
5. Because of the nature of the task, altitude rms error and elevator stick activity were strongly correlated while lateral offset rms error and aileron stick activity were not significantly correlated.

In general, the percentage improvement in performance was greatest for the situation for which the predictor element was primary (HSD). Beneficial improvements carried over to the secondary situation (VSD) as well.

#### FUTURE WORK SUGGESTIONS

While the experimental results unequivocally show the superiority of the predictor display in this type of simulation, it still remains to demonstrate its superiority in actual flight conditions and the relative magnitude of performance improvement there.

The apparent reduction in stress level and work load which can be attributed to use of the predictor display should also be determined. It is reasonable to assume that decreased stress and work loads are desirable and beneficial to optimum performance in either inner or outer loop control for dealing with a wider range of contingencies than would otherwise be possible.



Altitude prediction should be evaluated in conjunction with the ground path prediction. Integration of altitude and track predictions would be useful in simplifying eye scan and permitting more rapid evaluation of attitude and control corrections. Data of eye scan while using the predictor display elements would also be valuable information leading to an understanding of how they are used.

Better theoretical and practical understanding of the human's use of predictor information would allow more efficient design of predictor displays with the possibility of designing task-adaptive features to the displays. Man-Machine system modeling incorporating predictor elements should, therefore, be pursued. An early model of the human as a predictor can be found in Reference (9).

Use of predictor information in probability assessment should also be studied because of its relevance to the flight management situation.

## APPENDIX

### AIRCRAFT SIMULATION

The following equations and coefficients were used for the Navion aircraft dynamic simulation.

#### Airframe Dynamics

$$\begin{bmatrix} \dot{u} \\ \dot{w} \\ \dot{q} \end{bmatrix} = \begin{bmatrix} X_u & X_w & -g/s \\ Z_u & Z_w & U_0 \\ 0 & M_w & M_q \end{bmatrix} \cdot \begin{bmatrix} u \\ w \\ q \end{bmatrix} + \begin{bmatrix} 0 \\ Z_{\delta_e} \\ M_{\delta_e} \end{bmatrix} \cdot \delta_e$$

$$\dot{p} = L_p \cdot p + L_{\delta_a} \cdot \delta_a$$

$$Z_{\delta_e} = -8.45 \text{ ms}^{-2}$$

$$U_0 = 53.0 \text{ s}^{-1}$$

$$M_{\delta_e} = -11.1897 \text{ s}^{-2}$$

$$L_p = 8.402 \text{ s}^{-1}$$

$$X_w = 0.03607 \text{ s}^{-1}$$

$$L_{\delta_a} = 23.984 \text{ s}^{-2}$$

$$X_u = -0.0451 \text{ s}^{-1}$$

$$M_w = -0.0166 \text{ ms}^{-1}$$

$$Z_w = -2.0244 \text{ s}^{-1}$$

$$M_q = -2.0767 \text{ s}^{-1}$$

$$Z_u = -0.03697 \text{ s}^{-1}$$

The yaw rate ( $r$ ) was approximated for small bank angles by

$$\dot{z} = p \cdot \frac{z}{U_0}$$

#### ACKNOWLEDGEMENT

This research was supported through a NASA-ASEE 1971 Summer Faculty Fellowship with Mr. Thomas Wempe as the Research Supervisor. This support is very gratefully acknowledged as well as all the assistance provided by the Ames Research Center.

#### REFERENCES

1. Warner, J. D., "Advanced Controls and Displays for Future Commercial Aircraft Operations," AIAA 2nd Aircraft Design and Operations Meetings, Los Angeles, July 20-22, 1970. Paper No. 70-938.
2. Warner, J. D., "Advanced Display Systems for New Commercial Aircraft," Human Factors Society 14th Annual Meeting. San Francisco, California, October 12-16, 1970.
3. Ziebolz, H. and Paynter, H. M., "Possibilities of a Two-Time Scale Computing System for Control and Simulation of Dynamic Systems," Proceedings of the National Electronic Conference. Vol. 9, February 1954, pp. 215-223.
4. Kelley, C. R., "Manual and Automatic Control," Wiley & Sons, New York, 1968.
5. Warner, J. D. and Fadden, D. M., "Computer-Generated Map Displays," FAA Symposium on Area Navigation. Washington, D.C., January 24-25, 1972.
6. Dey, D., "Prediction Displays: A Simple Way of Modeling," Control Engineering, 8, July 1969, pp. 82-85.
7. Dey, D., "Results of the Investigation of Different Extrapolation Displays," Advanced Study Institute on Displays and Controls. Berchtesgaden, March 15-26, 1971.
8. Palmer, E. and Wempe, T., "Pilot Performance With a Simulated ILS-Independent Pictorial Display." 7th Annual Conference on Manual Control. NASA SP-281, 1971.
9. Kreifeldt, J. G., "Analysis of a Predictor Model," NASA CR 62006, July 1964.

# PILOT QUESTIONNAIRE

The responses to each question are paraphrased without altering their intent. Replies that appeared basically the same are reported as one entry. The number of replies if greater than one is noted next to each entry.

Replies were quite extensive in some cases with supporting pencil illustration.

- (1) Did you use the predictor display to a significant degree?

All pilots answered affirmatively.

- (2) What difficulties (if any) did it help you to cope with?

Eased turning and crosswind complications, provided instantaneous heading corrections, could anticipate turns and maintain track. Solved intercept angle and wind crab correction, prevented correcting in the wrong direction, aided in determining the correct bank angle.

- (3) What did you like about the PD?

Allowed an ease-off on scan while flying on heading. Convenience. Could see future course under present control action. Removed guesswork in track interception. Permitted easy navigation of a prescribed course.

- (4) What did you dislike about the PD?

Length of predicted path too long for display aircraft. Nothing. Requires too much scan away from horizon. Initial "whipping" (due to large, frequent control motions) initially disturbing. However, excellent behavior with gentle control. Aircraft symbol should always appear to move toward the top of the CRT.

- (5) What was your strategy in using the PD (i.e., how did you use it)?

Keep predicted path on the course to be flown. Fly the far end, once on track, on straight sections. On turns, keep the predictor going through the desired point until the aircraft arrives. Anticipated turns to rollout on proper course in order to maintain or correct track.

- [2] To remove control-display incompatibility in head-down positions.

The tip of the predicted path was used for its error magnification properties.

In turns, the far end of the predictor was set tangent to or coincident with the course line.

- (6) What information did the PD make available?

- [4] Advance track information under present control action. Future error.

- (7) How would you improve the PD?

Shorten predicted path to 1/4 length. Feed changing drift information into the predictor. No changes. Make it a command function at pilot's discretion. Larger A/C symbol on map. Rotatable map area.

- (8) What additional information would you want for flying the simulator

- (a) Without the PD?

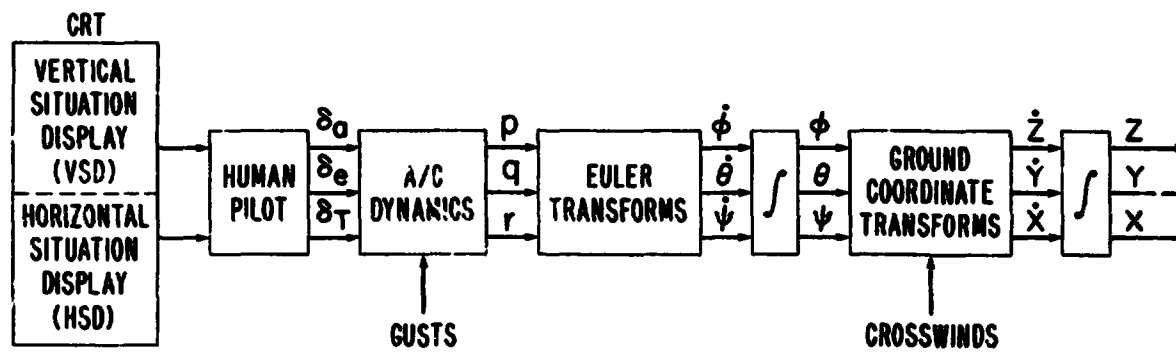
- (b) With the PD?

Suggestions common to both (a) and (b) are so noted

- (a,b) - Different colors for both A/C wings and error box in VSD. Hack marks at turn points on track. Curved track.  
[2] Rotatable map.

- (a) - Differently colored "single scan" display of altitude indicator ~~command~~ and steer indicator command.  
[2] Heading indicator.  
Bank angle in degrees.  
Crab angle indicator.

- (b) - Nothing.



ACTIVITY	RATE	ANGLE
$\delta_a$ = AILERON	$p$ = ROLL	$\phi$ = BANK
$\delta_e$ = ELEVATOR	$q$ = PITCH	$\theta$ = PITCH
$\delta_T$ = THROTTLE	$r$ = YAW	$\psi$ = YAW
	(SHIP COORDINATES)	(INERTIAL COORDINATES)

Figure 1. Functional block diagram of the human operator and the system transformations.

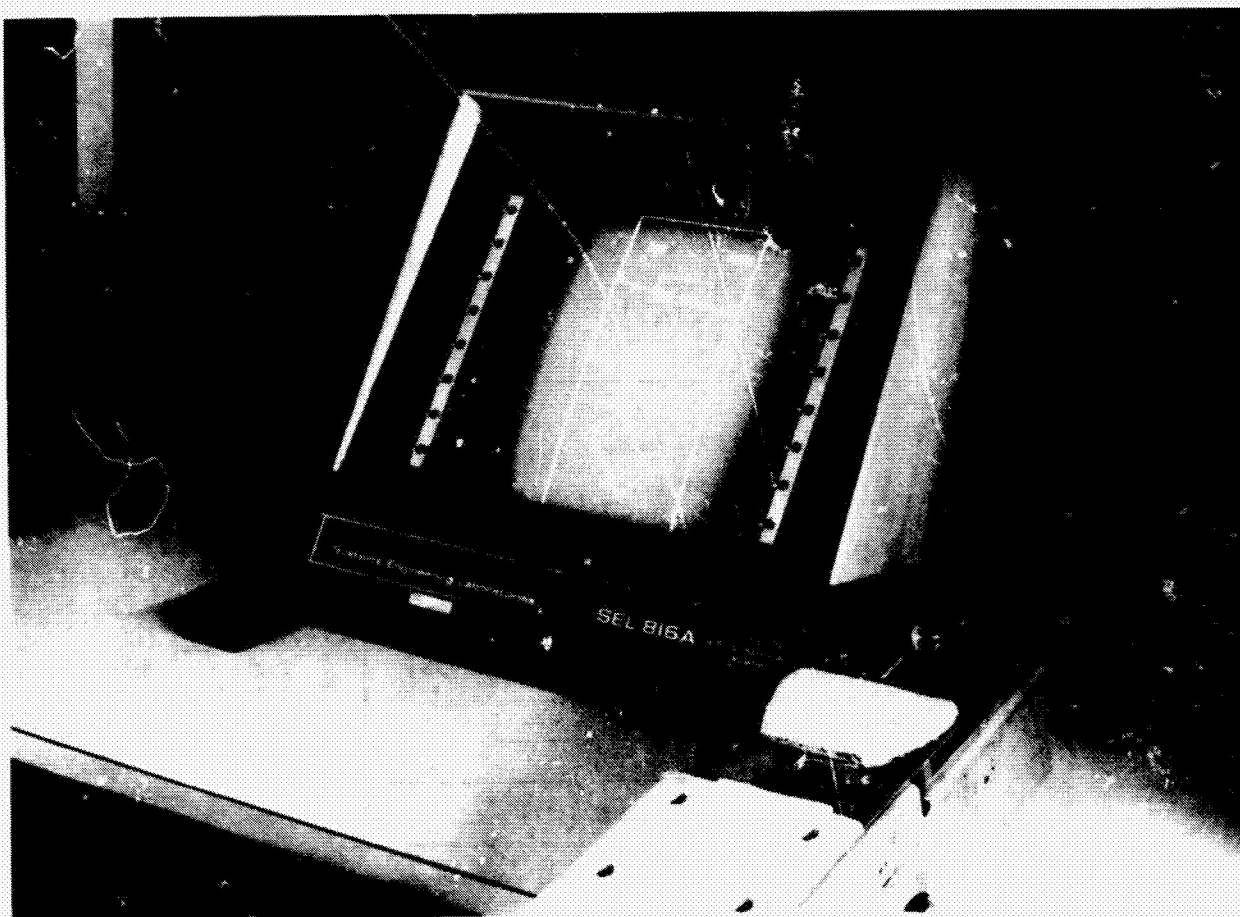


Figure 2. Photograph of the basic simulation configuration.

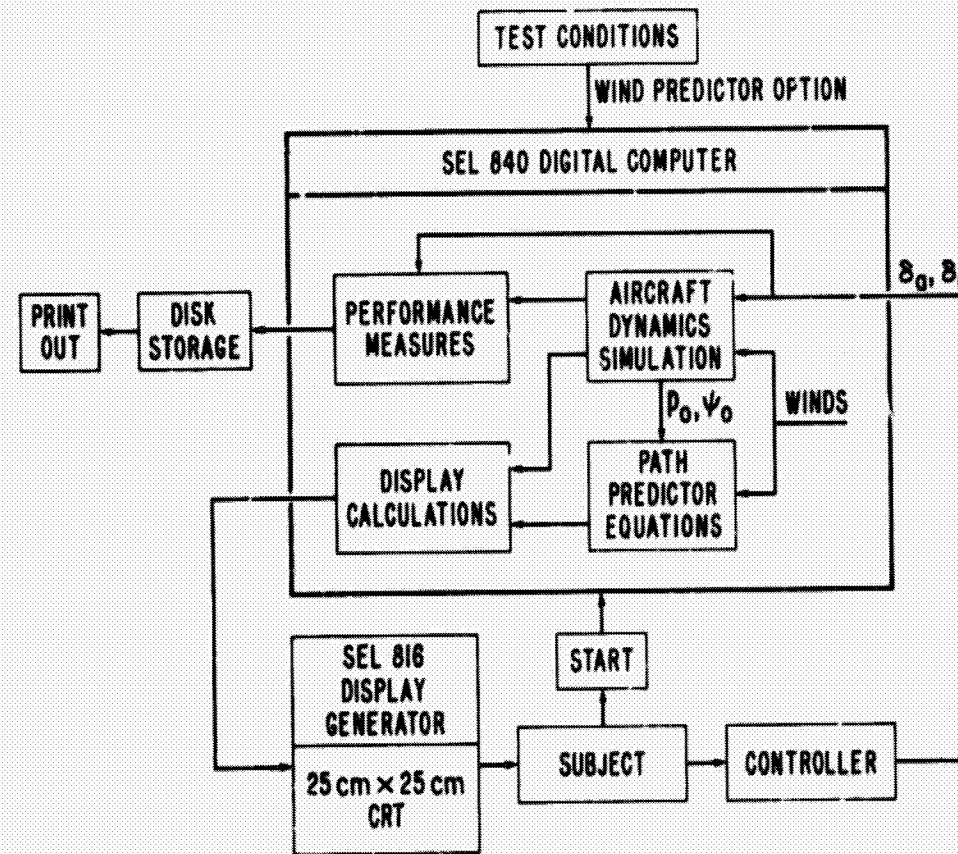


Figure 3. Functional block diagram of the experimental configuration.

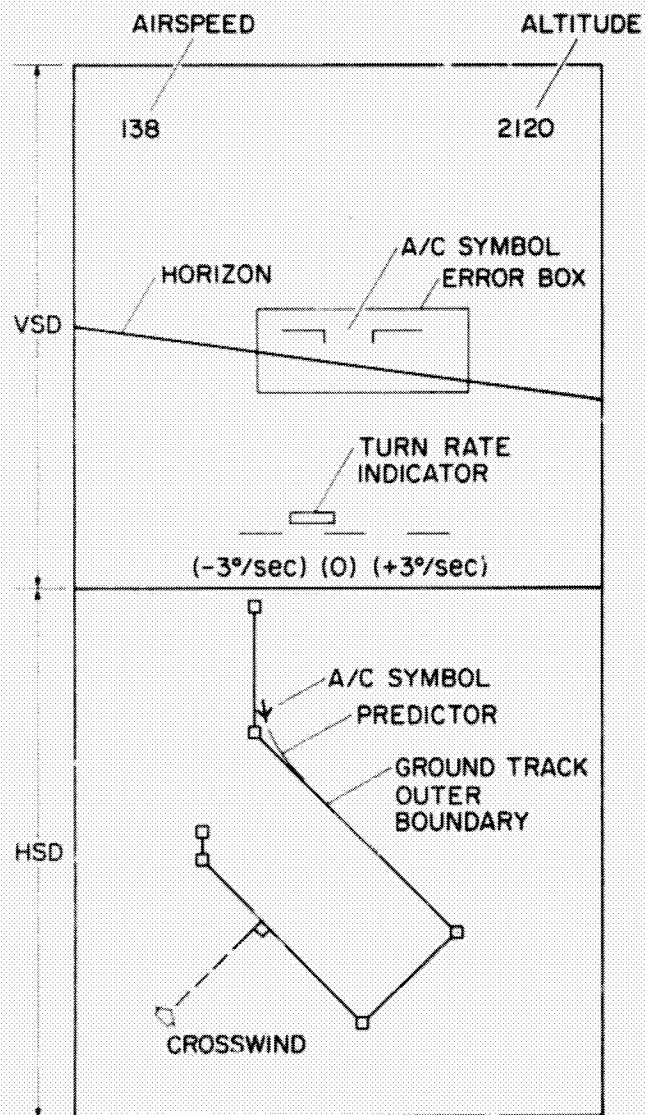


Figure 4. A labeled photograph of the CRT display showing the horizontal and vertical situation displays and the crosswind direction.

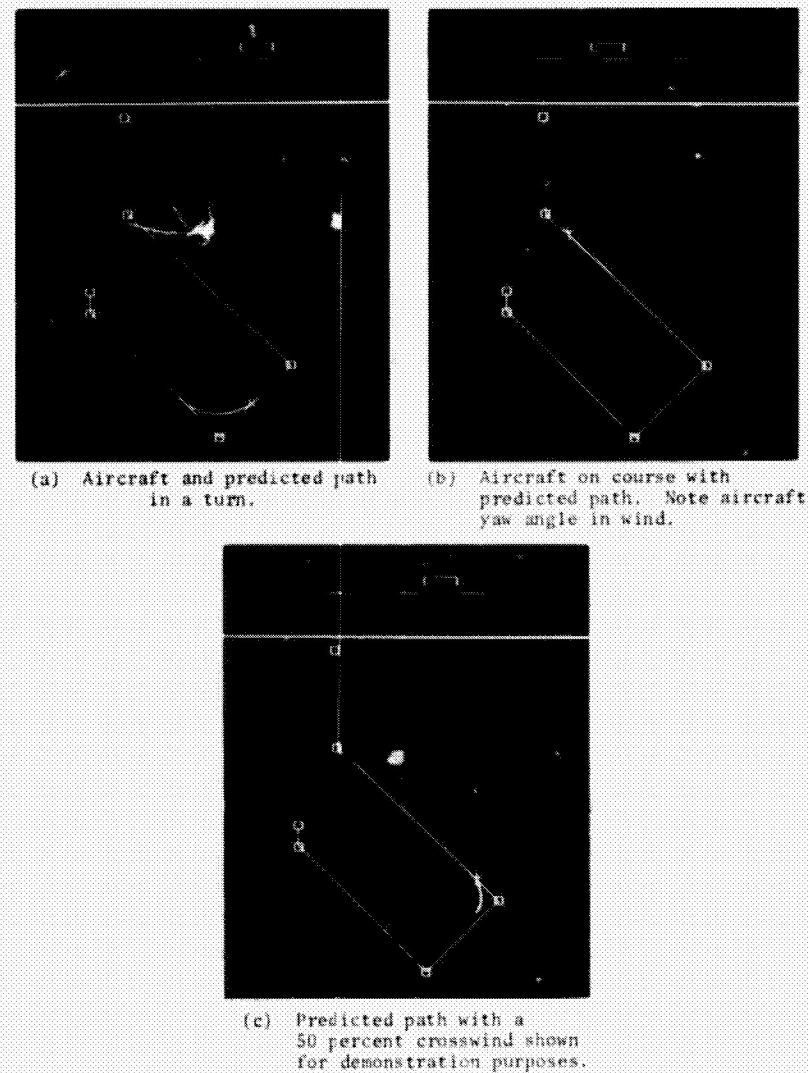


Figure 5. Horizontal situation display

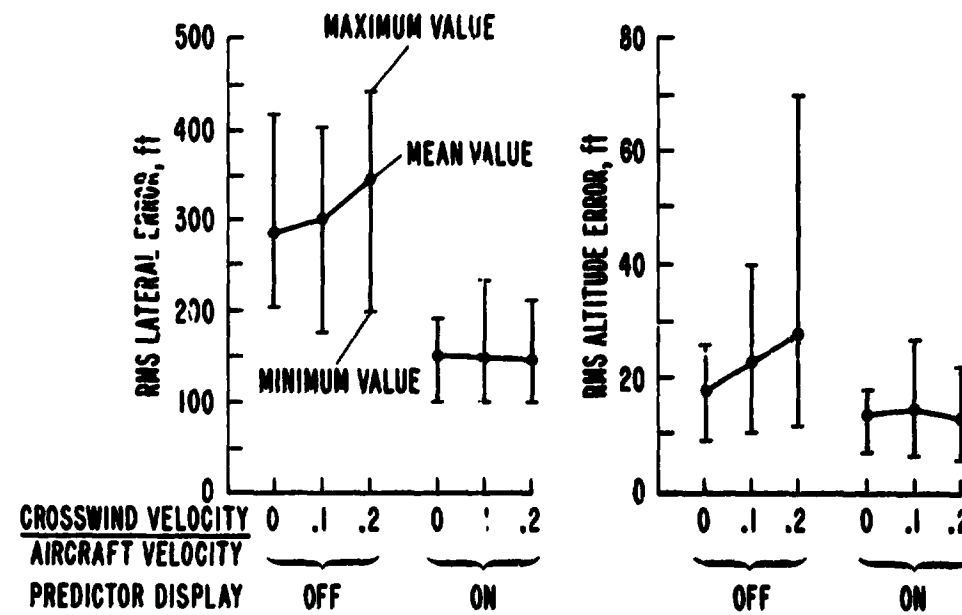


Figure 6. Pilot performance during a standard instrument procedure turn with and without a ground track predictor display. RMS lateral and altitude error.